Received: 17 October 2018 | Accepted: 1 April 2019

DOI: 10.1002/kjm2.12072

ORIGINAL ARTICLE

Kaohsiung Journal of Medical Sciences KJMS Open Access WILEY

Klotho/FGF23 axis mediates high phosphate-induced vascular calcification in vascular smooth muscle cells via Wnt7b/β-catenin pathway

Yan-Xia Chen | Chong Huang | Zhi-Bing Duan | Cheng-Yun Xu | Yan Chen

Department of Nephrology, The Second Affiliated Hospital of Nanchang University, Nanchang, China

Correspondence
Yan Chen, Department of Nephrology, The Second Affiliated Hospital of Nanchang University, No.1, Minde Road, Donghu District, Nanchang 330006, Jiangxi Province, China.
Email: chenyanabc@163.com

Funding information
Key Research and Development Projects of Jiangxi Science and Technology Department, Grant/Award Number: 20171BBG70071

Abstract

Vascular calcification (VC) plays as a critical role on cardiovascular disease (CVD) and acts as a notable risk factor in cardiovascular system. Vascular smooth muscle cells (VSMCs) calcification can be triggered by high phosphate treatment; however, the explicit mechanism remains unclear. In the present study, we isolated VSMCs from primary rat artery, applied β-GP (β-glycerophosphate) for inducing VSMCs calcification in vitro to explore the mechanism of phosphate-induced calcification in VSMCs. Alizarin red staining was performed to assess the mineralization in VSMCs. Calcium deposition experiment was taken to evaluate the calcium content. ALP staining was determined to assess the ALP activity. The recombinant adenoviruses were constructed for the overexpression of Klotho and FGF23, respectively. qRT-PCR and western blot analysis were subjected to measure the expression of Klotho/FGF23 and correlated genes among Wnt7b/β-catenin pathway. We found that the calcium content was obviously increased and Alizarin red staining was positive in calcification group exposure with high phosphate in a time-dependent manner. The expression of Klotho and FGF23 was significantly decreased in the calcification group. However, overexpression of Klotho and FGF23 markedly reversed VSMCs calcification stimulating with high phosphate treatment. Moreover, Wnt7b/β-catenin inhibitor DKK1 could partly attenuate the effect of high phosphate on calcified VSMCs. These findings demonstrated that Klotho/FGF23 axis could modulate high phosphate-induced VSMCs calcification via Wnt7b/β-catenin signaling pathway. Our findings unravel that Klotho/FGF23- Wnt7b/β-catenin axis functions as a crucial role in the VSMCs calcification.

KEYWORDS
FGF23, high phosphate, Klotho, vascular calcification, Wnt7b/β-catenin

1 | INTRODUCTION

Patients with chronic kidney disease (CKD) show an increasing risk of severe cardiovascular diseases (CVD).[1,2] Cardiovascular diseases account for 30% to 50% of all-cause mortality in patients with CKD and end-stage kidney disease worldwide.[3,4] Although various risk factors contributed to cardiovascular complications are well recognized during the development of CKD, it is still unable to explain the specific molecular mechanisms of placing a premium on cardiovascular disease.

Vascular calcification (VC) is very common and, at present, it is one of the main complications of CKD, which increases the CVD related mortality.[5,6] The formation of VC is associated with complex pathological mechanisms, including osteochondral differentiation and apoptosis of vascular smooth muscle cells (VSMCs), instability and release of extracellular vesicles loaded calcium and phosphate.[1,7] Among the various causes in CKD, abnormal deposition of calcium phosphate (Pi) salt is most closely related to VC.[8] It has been proved that elevated serum Pi is a risk factor for VC and cardiovascular mortality and morbidity among CKD populations in clinical studies.[9,10] Therefore, it is of great significance to study the specific molecular mechanism of VSMCs calcification induced by high phosphorus in CKD.

Recently, it has been reported that Klotho and Fibroblast growth factor-23 (FGF23) in the field of CKD was closely related to Pi homeostasis.[11] The Klotho gene encodes a 130-kDa single-channel transmembrane protein with a short cytoplasmic domain (10 amino acids) that is primarily expressed in the kidney.[12,13] FGF23 was identified as a phosphaturic hormone and mainly produced by osteocytes in the bone.[14,15] Klotho significantly enhances the ability of FGF23 and functions as a cofactor essential for activation of FGF signaling by FGF23.[12] Besides, Klotho was identified to function as a role in vascular calcification. Lim et al. found that vascular Klotho deficiency potentiates the development of human artery calcification and mediates resistance to FGF23.[16] However, the role of FGF23 in vascular calcification is currently inconclusive.

The Wnt/β-catenin pathway is a family of proteins that is implicated in many vital cellular functions such as vascular calcification.[17,18] Among recent reports, Yao et al. revealed that high phosphorus level leads to aortic calcification via β-catenin in CKD.[17] Besides, VC in CKD was also reported to be induced via a mechanism involving the Wnt/β-catenin pathway.[18] However, whether the Klotho/FGF23 axis regulates the relevant signaling molecules in Wnt/β-catenin signaling, and then mediates the osteogenic differentiation and calcification of VMSC has not been reported.

In this study, we demonstrated that the expression of Klotho and FGF23 was reduced by high phosphate-induced VSMCs calcification and the overexpression of Klotho and FGF23 could reverse high phosphate-induced VC. Furthermore, we found that Klotho and FGF23 attenuated phosphate-induced vascular calcification through inhibiting Wnt7b/β-catenin pathway. Additionally, our results identified that Klotho/FGF23-Wnt7b/β-catenin may act as a novel therapeutic target of vascular calcification.

2 | METHODS

2.1 | Cell extraction, cell culture and reagents

Primary rat aortic VSMCs were employed for this study. The primary rat aortic VSMCs were extracted and cultured as described.[6] Briefly, Male Sprague-Dawley (SD) rats (150-180 g, 10-12 week) were ordered from the Laboratory Animal Center of Chongqing Medical University. All animal experiments were approved by the institutional animal care and use committee (IACUC). The intima and adventitia were memoved carefully. Then, collected the arota and cut into small sections.

The primary rat aortic VSMCs were cultured in DMEM supplemented with 10% fetal bovine serum (FBS, Gibco), 100 U/mL of penicillin and 100 μg/mL of streptomycin at 37°C under 5% CO_2 and 95% ambient air.

All primary antibodies were ordered from Santa Cruz Biotechnology (Santa Cruz, CA, USA). Wnt inhibitor DKK1 was purchased from Sigma-Aldrich (St. Louis, Missouri). β-GP (β-glycerophosphate) for inducing VSMCs calcification in vitro was ordered from Sigma-Aldrich.

2.2 | Induction of VSMCs calcification

VSMCs were routinely subcultured in DMEM growth medium. When VSMCs were at 70% to 80% confluence in the media, the cells were switched to calcification medium (DMEM growth medium containing 10 mM β-GP) for indicated intervals. The medium was replaced every 3 days. For time course experiments, the first day of culture in the calcification medium was defined as Day 0.

2.3 | Alizarin red staining

The cells were fixed with 70% ice-cold ethanol for 1 hour and rinsed with double-distilled H_2O, and then were stained with 40 mM Alizarin red S (pH 4.9, Sigma-Aldrich) for 15 minutes at room temperature. After staining, the cells were washed five times with double-distilled H_2O. For the quantitative assessment of the degree of mineralization, the red stain was eluted by 10% (wt/vol) cetylpyridinium chloride monohydrate (Sigma-Aldrich) for 1 hour and quantified via spectrophotometric absorbance measurements of the OD at 562 nm.

2.4 | Calcium deposit experiment

Calcium deposit experiment was determined with calcium kit. Cells were cleaved, centrifuged, and 50μl of supernatant was taken. The detection reagent was added to determine the OD value at 610 nm. Total protein content in cells was detected by BCA protein quantitative kit. The content of Ca^{2+} in cells was calculated according to OD value, standard product concentration and protein concentration of samples to be measured in each group, and the content was expressed as mmol/g protein.

2.5 | Quantitative real-time PCR

According to the manufacturer's instructions, TRIzol reagent (Invitrogen, Carlsbad, California) was using for isolating the total RNA of cells. First-strand cDNA was synthesized from 1 μg of total RNA by incubation for 1 hour at 42°C with Superscript III reverse transcriptase (Invitrogen) following oligo (dT) priming. After the reverse transcription reaction, an ABI 7900HT system using SYBR Premix (Takara, Dalian, China) was applied to measure the real-time polymerase chain reaction (RT-PCR) according to the manufacturer's instructions. The conditions for RT-PCR were as follows: denaturation at 95°C for 10 seconds and 40 cycles of 95°C for 10 seconds and 60°C for 30 seconds. A dissociation stage was added to the end of the

amplification procedure. No nonspecific amplification was observed, as determined using the dissociation curve. Glyceraldehyde 3-phosphate dehydrogenase (GAPDH) was used as an internal control. The data were analyzed using the comparison Ct ($2^{-\Delta\Delta Ct}$) method and expressed as the fold change relative to the respective control. Each sample was analyzed in triplicate.

2.6 | Construction of recombinant adenoviruses for Klotho and FGF23

The recombinant adenoviruses were constructed following the AdEasy system.[6] Briefly, the coding sequence (CDS) of human Klotho and FGF23 were amplified. These fragments were sub-cloned into shuttle vectors, respectively. Then, the shuttle vectors were linearized and transfected into HEK293 cells for packaging recombinant adenovirus, which were designated as Ad-Klotho and Ad-FGF23. The recombinant adenovirus expressing AdLaz only was used as vector control. All these recombinant adenoviruses were purchased from Addgene (Cambridge, Massachusetts).

2.7 | Small interfering RNA transfection

Klotho or FGF23 shRNA and a negative control were purchased from GenePharma (Shanghai, China). For transfection, cells were cultured in six-plates by using Lipofectamine 2000 (Invitrogen), according to the manufacturer's instructions. The sense strand of Klotho shRNA was as follows: 5′-CCGGCAAGGCATCCATGAAACATTACTCGAGTAATGTTTC ATGGATGCCTTGTTTTTTG-3′. The sense strand of FGF23 shRNA was as follows: 5′-CCGGTCCTCAGAGCCTATCCCAATGCTCGAGCATTGGG ATAGGCTCTGAGGATTTTTG-3′.

2.8 | Alkaline phosphatase staining and activity assay

ALP staining assay was determined as reported.[19] ALP staining was performed on cultured control and β-GP-treated cells. After being rinsed with PBS three times, the cell layer was fixed in 4% paraformaldehyde for 15 minutes at room temperature. And then the cells were incubated with buffer containing 0.1% naphthol AS-Bi phosphate (Sigma-Aldrich) and 2% fast violet B (Sigma-Aldrich). After incubation for 1 hour at 37°C, the cell layer was washed with deionized water. An ALP activity assay was performed at 405 nm using p-nitrophenyl phosphate (pNPP) (Sigma Aldrich) as the substrate. Briefly, a 50 mL sample was incubated with 50 mL of pNPP (1 mg/mL) in 1 M diethanolamine buffer containing 0.5 mM $MgCl_2$ (pH 9.8) at 37°C for 15 minutes. The reaction was stopped by adding 2 M NaOH to 200 μL of the reaction mixture. BCA method with a protein assay kit (PIERCE, Rockford, Illinois) was performed to detect the total protein content and ALP activity was determined as nmol p-nitrophenol per minute per mg protein and presented as the fold change relative to that of the control group.

2.9 | Western blot analysis

We collected the cells from the plates and then used lysis buffer supplemented with protease inhibitors (10 mg/mL leupeptin, 10 mg/mL pepstatin A, and 10 mg/mL aprotinin) for extracting total protein about 30 minutes. Protein samples were collected by centrifugation at 15 000g at 4°C for 10 minutes. Then the Micro Bicinchoninic acid (BCA) Assay Kit (Thermo Fisher Scientific, Waltham, MA, USA) was using for determining protein concentrations. In addition, 20 μg of total protein extract was then subjected to 10% or 12% sodium

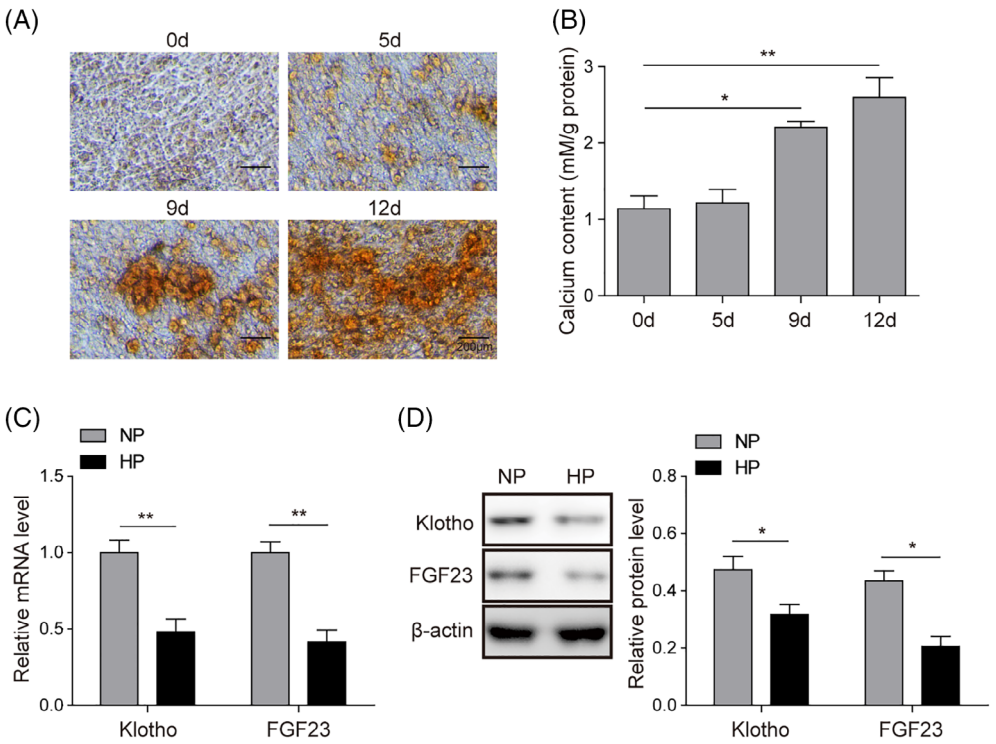

FIGURE 1 The expression of Klotho and FGF23 in VSMCs calcification induced by high phosphate treatment. A, Alizarin red S staining was performed to detect mineralization in VSMCs with β-GP treatment for 0, 5, 9, or 12 days. Scale bar, 200 μm. B, the calcium content of VSMCs with β-GP treatment for 0, 5, 9, or 12 days. *$P < .05$ and **$P < .01$ vs 0 day. C, qRT-PCR assay was performed to detect the mRNA expression of Klotho and FGF23 in VSMCs with or without high phosphate treatment. **$P < .01$ vs NP. D, Western blot analysis of the protein expression of Klotho and FGF23 in VSMCs with or without high phosphate treatment. *$P < .05$ vs NP. NP, normal phosphate; HP, high phosphate; VSMCs, vascular smooth muscle cells

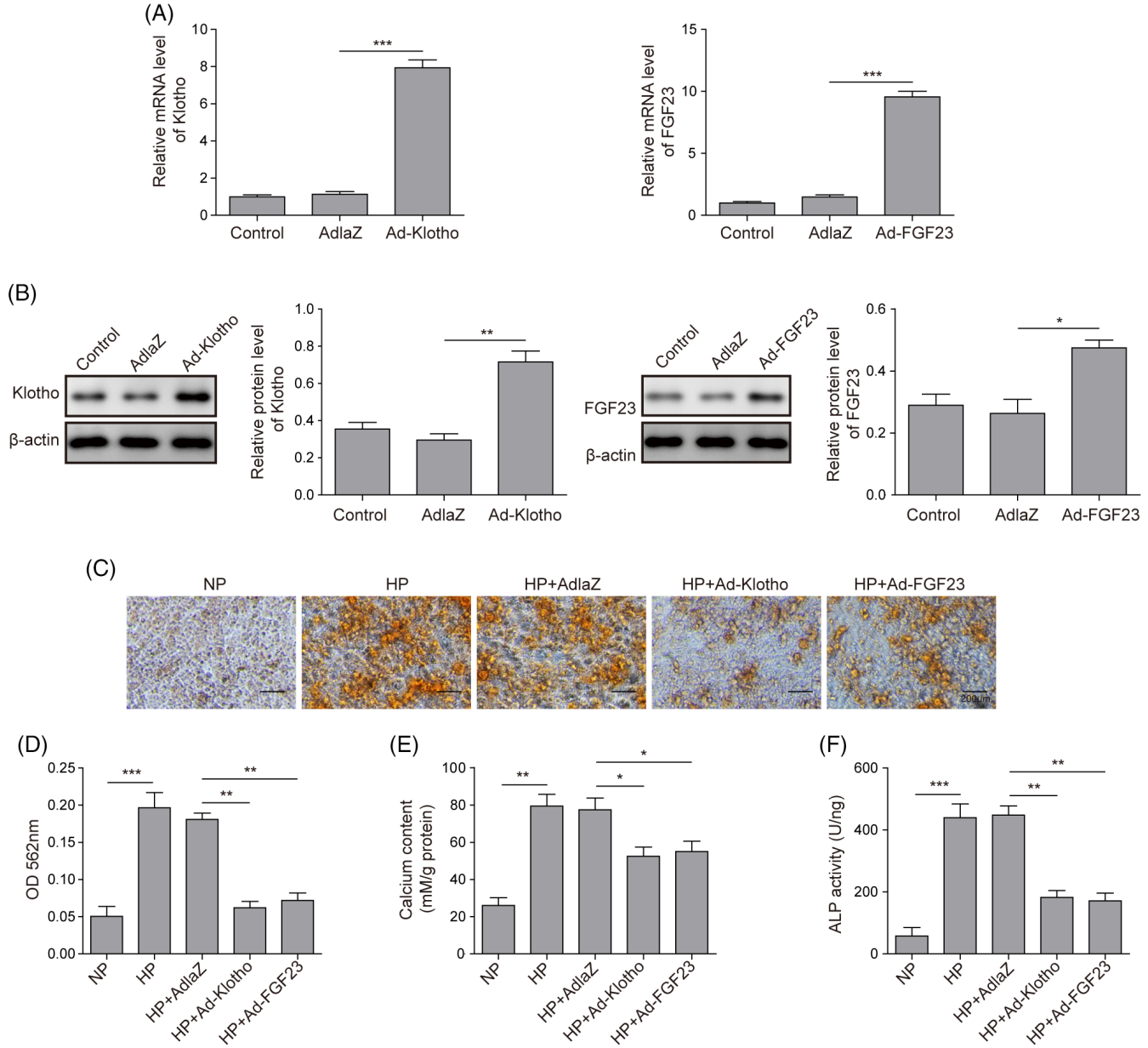

FIGURE 2 Overexpression of Klotho and FGF23 relieved high phosphate-induced VSMCs calcification. A-B, VSMCs infected with recombinant adenovirus expressing Klotho or FGF23 and the overexpressing efficiency of Klotho or FGF23 was detected by qRT-PCR and western blot, respectively. **P* < .05,***P* < .01 and ****P* < .001 vs AdlaZ. VSMCs were divided into five groups as follows: Normal VSMCs (NP); VSMCs treated with β-GP for 12 days (HP); VSMCs infected with AdlaZ and treated with β-GP for 12 days (HP+ AdlaZ); VSMCs infected with recombinant adenovirus expressing Klotho and treated with β-GP for 12 days (HP+ Ad-Klotho); VSMCs infected with recombinant adenovirus expressing FGF23 and treated with β-GP for 12 days (HP+ Ad-FGF23). C, Alizarin red S staining was performed to detect mineralization and representable pictures was shown. Scale bar, 500 μm. D, Quantification results for the alizarin red S staining. ****P* < .001 vs NP and ***P* < .01 vs HP + AdlaZ. E, The calcium content of VSMCs in five groups. ***P* < .01 vs NP and **P* < .05 vs HP + AdlaZ. F ALP activity of VSMCs in five groups. ****P* < .001 vs NP and ***P* < .01 vs HP + AdlaZ. NP, normal phosphate; HP, high phosphate; VSMCs, vascular smooth muscle cells

dodecyl sulfate-polyacrylamide gel electrophoresis (SDS-PAGE) and transferred to nitrocellulose membranes (Whatman, Piscataway, New Jersey). After being blocked with 5% BSA, the membranes were incubated with according antibodies overnight at 4°C. A horseradish peroxidase-conjugated secondary antibody was added and visualized using an enhanced chemiluminescence detection system (Millipore, Billerica, Massachusetts) as recommended by the manufacturer.

2.10 | Statistical analysis

Statistic comparisons between results from multiple groups were analyzed using one-way analysis of variance (ANOVA) followed by Dunnett's test. For experiments involving two groups, an unpaired Student's *t*-test was performed. A value of $P < .05$ was considered statistically significant. Data are expressed as mean ± standard deviation (SD). A *P*-value < .05 was considered statistically significant.

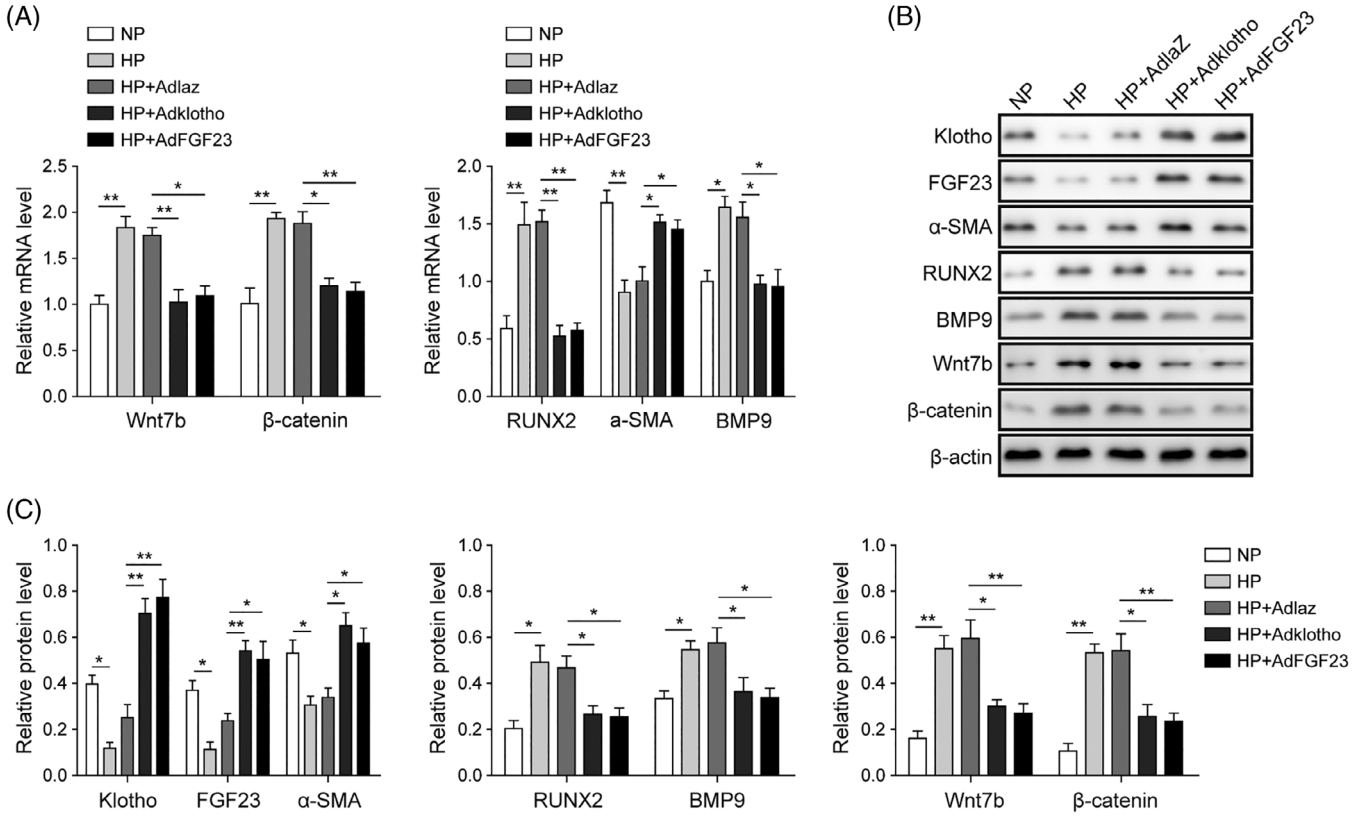

FIGURE 3 High phosphate facilitate VSMCs calcification through activating Wnt7b/β-catenin signaling pathway. A, The mRNA expression levels of Runx2, α-SMA, BMP9, Wnt7b, and β-catenin were assessed by qRT-PCR. **P* < .05 and ***P* < .01 vs NP. **P* < .05 and ***P* < .01 vs HP + AdlaZ. B, The protein expression levels of Klotho, FGF23, α-SMA, Rnux2, BMP9, Wnt7b, and β-catenin were measured by western blot analysis. **P* < .05 and ***P* < .01 vs NP. **P* < .05 and ***P* < .01 vs HP + AdlaZ. NP, normal phosphate; HP, high phosphate; VSMCs, vascular smooth muscle cells

3 | RESULTS

3.1 | VSMCs calcification induced by high phosphate suppressed Klotho and FGF23 expression

It is well-known that vascular calcification can be caused by high phosphate (HP), therefore, we firstly establish a VSMCs calcification model by β-GP (β-glycerophosphate) treatment. As shown in Figure 1A, alizarin red S staining results showed that β-GP induced mineralized nodules in VSMCs in a time-dependent manner. In line with this observation, we found that high phosphate enhanced the calcium content, suggesting β-GP treatment could induce VSMCs calcification (Figure 1B). To further validate the effect of VSMCs calcification on Klotho and FGF23, we assessed the mRNA and protein expression levels using qRT-PCR and western blot analysis. As shown in Figure 1C,D, β-GP induction suppressed the mRNA and protein expression of Klotho and FGF23. These results indicated that high phosphate treatment might promote VSMCs calcification through regulating the expression of Klotho and FGF23.

3.2 | Overexpression of Klotho and FGF23 alleviated high phosphate-induced VMSCs calcification

To further validate whether Klotho and FGF23 were involved in the vascular calcification induced by HP treatment, the expression levels of Klotho and FGF23 in VSMCs were overexpressed before exposure to β-GP. Moreover, the Alizarin Red S staining assay, calcium deposit experiment and ALP staining assay were also performed to determine their functions in vascular calcification. Firstly, the overexpressing efficiency of Klotho or FGF23 was examined using qRT-PCR and western blot. As shown in Figure 2A,B, the mRNA and protein levels of Klotho and FGF23 were both obviously up-regulated. Then, further functional experiments showed that high phosphate stimulation enhanced VSMCs calcification, while overexpression of Klotho or FGF23 with recombinant adenovirus both reversed the mineralized nodule formation increased by HP (Figure 2C,D). Consistently, overexpression of Klotho and FGF23 also reduced the calcium content and inhibited ALP activity which were elevated by phosphate incubation (Figure 2E,F). Therefore, these data indicated that Klotho and FGF23 might be involved in mediating the VSMCs calcification induced by high phosphate.

3.3 | High phosphate facilitated VSMCs calcification through activating Wnt7b/β-catenin pathway

To gain insight into the explicit molecular mechanism underlying the vascular calcification induced by HP, we further examined whether HP enhanced VSMCs calcification via regulating Wnt7b/β-catenin pathway. Firstly, we determined the expression of Wnt7b/β-catenin signals using quantitative real-time PCR (qRT-PCR) assay. The results showed that

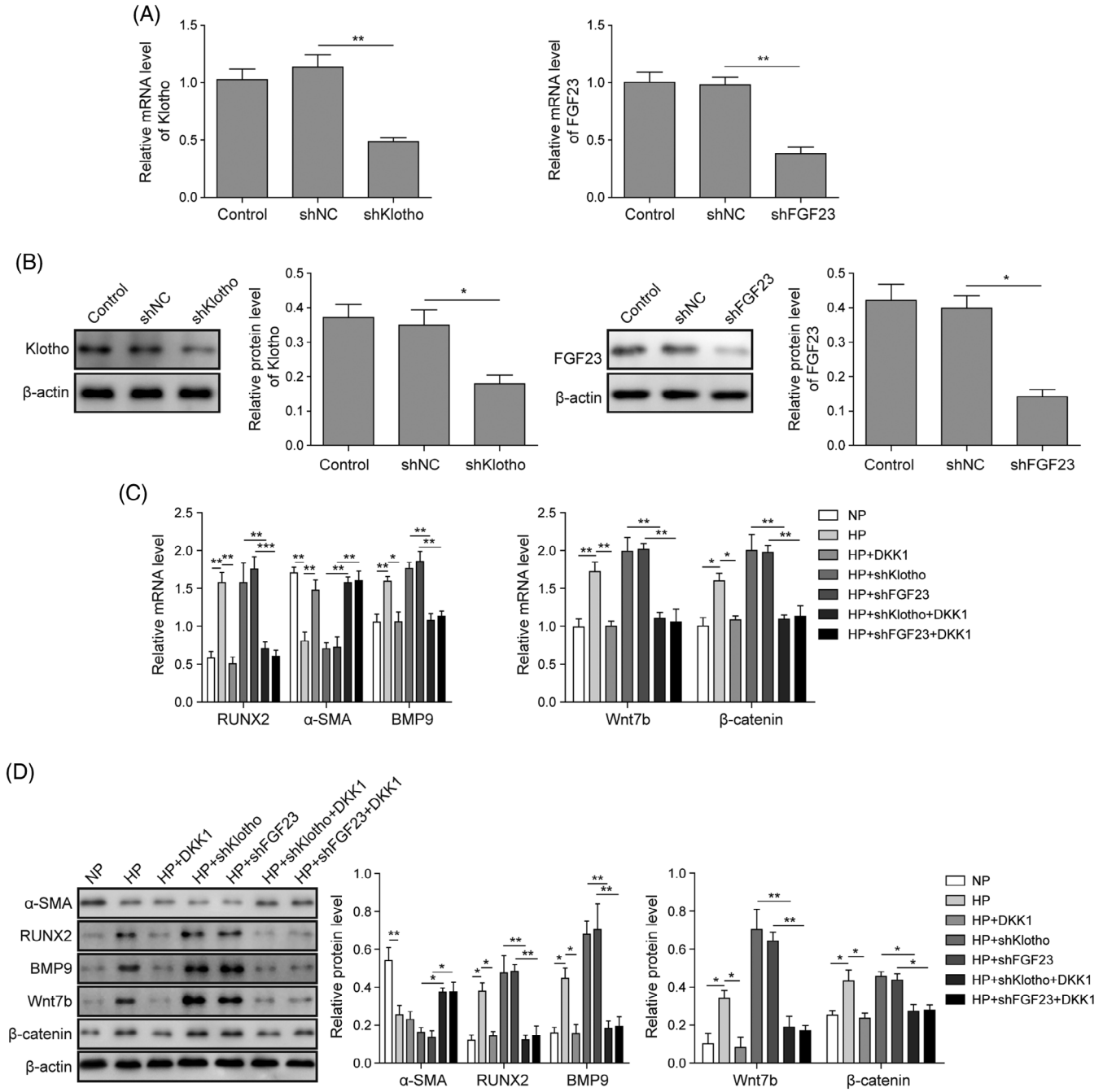

FIGURE 4 Klotho and FGF23 alleviates phosphate-induced VSMCs calcification through inhibiting Wnt7b/β-catenin signaling pathway. A-B, The silencing efficiency of Klotho or FGF23 was determined by qRT-PCR and western blot, respectively. *P < .05 and **P < .01 vs shNC. C, Cells were pretreated with DKK1 (an inhibitor of Wnt7b/β-catenin signaling) and then the mRNA expression levels of Runx2, α-SMA, BMP9, Wnt7b, and β-catenin were determined by qRT-PCR assay. *P < .05 and **P < .01 vs NP. *P < .05 and **P < .01 vs HP. **P < .01 vs HP + shKlotho. **P < .01 and ***P < .001 vs HP + shFGF23. D, Western blot analysis was subjected to assess the protein expression levels of α-SMA, Rnux2, BMP9, Wnt7b, and β-catenin. **P < .01 vs HP + shKlotho. *P < .05 vs HP. *P < .05 and **P < .01 vs HP + shKlotho. *P < .05 and **P < .01 vs HP + FGF23. NP, normal phosphate; HP, high phosphate; VSMCs, vascular smooth muscle cells

HP up-regulated the mRNA expression levels of Wnt7b, β-catenin, Runx2, and BMP9, while significantly inhibited alpha-smooth muscle cell actin (α-SMA) expression. On the contrary, either Klotho or FGF23 upregulation both restrained the mRNA levels of Wnt7b, β-catenin, Runx2, and BMP9 induced by HP treatment but promoted α-SMA mRNA expression (Figure 3A). Similar findings were confirmed by western blot analysis. As shown in Figure 3B, upregulation of Klotho and FGF23 blocked the increasing levels of Runx2, BMP9, Wnt7b, and β-catenin protein levels induced by HP stimulation, and reversed the downregulation of α-SMA protein expression. In summary, these findings indicated that Wnt7b/β-catenin pathway might get involved in the vascular calcification induced by high phosphate.

3.4 | Klotho and FGF23 attenuated phosphate-induced VSMCs calcification through inhibiting Wnt7b/β-catenin pathway

As Klotho has been reported to act as a suppressor of the Wnt/β-catenin pathway,[20] we next explored whether Klotho/FGF23 has a critical role in phosphate-induced VSMCs calcification via inhibiting Wnt7b/β-catenin pathway. We first determined the expression of Wnt7b/β-catenin pathway in VSMCs silenced by shKlotho/shFGF23 with or without Wnt7 inhibitor DKK1 in the treatment of HP. The silencing efficiency of Klotho and FGF23 was confirmed using qRT-PCR and western blot (Figure 4A, B). Besides, the relative expression levels of vascular calcification related proteins and Wnt7b/β-catenin signals were further investigated. As shown in Figure 4C,D, VSMCs cultured with DKK1 promoted α-SMA, and inhibited the expression of Runx2, BMP9, Wnt7b, and β-catenin which were increased by HP. Furthermore, DKK1 treatment also rescued an augment of Wnt7b/β-catenin pathway induced by the knockdown of Klotho/FGF23 using shKlotho and shFGF23. Taken together, these data indicated that Klotho/FGF23 attenuated phosphate-induced vascular calcification through inhibiting Wnt7b/β-catenin pathway.

4 | DISCUSSION

The Klotho/FGF23 axis is identified as a target for kidney clinics, and Klotho/FGF23 is a prognostic biomarker for CKD and CVD.[15] The presence of Klotho in vascular walls is unclear; however, all the experiments have shown that Klotho prevents VC development. Hu et al. found that Klotho deficiency in CKD mice leads to VC.[21] Lim et al. found that vascular Klotho deficiency potentiates the development of human artery calcification.[16] Zhao et al. reported that inhibition of mammalian target of rapamycin signaling suppresses VC in CKD via up-regulating membrane bound vascular α-Klotho.[22] These results suggest that Klotho is the potential therapeutic target of VC in CKD. However, the potential effects of FGF23 on VC remain unclear. Jimbo et al. reported that FGF23 accelerates phosphate-induced vascular calcification in the absence of Klotho deficiency.[23] However, Massy et al. suggested that the disturbances of the FGF23/Klotho axis observed in CKD appears to play an important role in CKD-associated VC.[24] FGF23 was also reported as an independent biomarker of vascular calcification in patients with various CKD stages including early stages.[25] In this article, we revealed that the expression of Klotho and FGF23 was reduced by high phosphate-induced VSMCs calcification and the overexpression of both Klotho and FGF23 could reverse high phosphate-induced VC, indicating that Klotho and FGF23 might play an important mediator on VSMCs calcification.

VC is an active and complex process involving the pathological deposition of mineral in the vascular system, including intimal calcification and medial calcification, which can also be found in the valves of the heart.[26] VC was previously considered as passive deposition of calcium salts, however, recent studies have found that VC, especially the medial calcification, is an active and controllable complex biological process similar to bone development, and the critical process of VSMCs calcification is the transition of an osteoblastoid phenotype.[27] This process, which has been seemed as the osteoblastic differentiation of VSMCs, accompany with the downregulation of VSMC-related markers, such as α-SMA and SM22α.[28] It is well-known that phosphate plays a vital role in the development of VSMCs calcification.[29,30] Thus, in the present study, we applied β-GP for inducing VSMCs calcification in vitro to explore the mechanism of VSMCs calcification. Similarly, our study also revealed that high phosphate induced VSMCs calcification, accompanied by the downregulation of VSMC markers (such as α-SMA) and upregulation of osteogenic markers (such as RUNX2). In addition, overexpression of Klotho and FGF23 could significantly reverse the negative effects of high phosphate, which increased the α-SMA expression and inhibited theRUNX2 expression. These findings identified Klotho/FGF23 signaling axis as a key role in VSMCs calcification.

Several important signal pathways have been activated in VC, such as BMPs/Smads and Wnt/β-catenin pathway. Wnt/β-catenin pathway recently was reported to be involved in VC, but whether it plays as an inducer or inhibitor was unclear. Liu et al. identified that increased activation of Wnt pathways in the arteries of patients with end-stage renal disease. And it is significantly correlated with the incidence of vascular calcification[31] Besides, Rong et al. reported that BMP-2 plays a crucial role both in calcium deposition in VSMCs and VC in CKD patients via a mechanism involving the Wnt/β-catenin pathway.[18] In addition, BMP-9 was also been reported to induce VC through activating the Wnt/β-catenin pathway.[6] In contrast, Deng et al. revealed secreted frizzled-related protein 5 (SFRP5) attenuates high phosphate-induced calcification in vascular smooth muscle cells by inhibiting the Wnt/β-catenin pathway.[32] Thus, Wnt/β-catenin pathway was generally identified as an inducer of vascular calcification, and regulated by several signal molecules, including BMP family and SFRP5. In this study, we suggested that vascular calcification was promoted by Wnt7b/β-catenin pathway in the presence of high phosphate. The treatment of Wnt inhibitor DKK1 rescued an augment of Wnt7b/β-catenin pathway induced by the knockdown of Klotho/FGF23.

In summary, we demonstrated that both Klotho and FGF23 reversed the VSMCs calcification induced by high phosphate. In addition, Klotho and FGF23 impaired phosphate-induced vascular calcification through inhibiting Wnt7b/β-catenin pathway. With these newly acquired mechanistic insights, this article provides "Klotho/FGF23-Wnt7b/β-catenin pathway" as a novel target for the prevention and treatment of VC.

CONFLICT OF INTEREST

All authors declare no conflicts of interests.

ORCID

Yan Chen https://orcid.org/0000-0003-3145-071X

REFERENCES

1. Yamada S, Giachelli CM. Vascular calcification in CKD-MBD: Roles for phosphate, FGF23, and Klotho. Bone. 2017;100:87–93.

2. Masakane I, Nakai S, Ogata S, Kimata N, Hanafusa N, Hamano T, et al. An overview of regular dialysis treatment in Japan (as of December 31, 2013). Ther Apher Dial. 2015;19(6):540–574.
3. Collins AJ, Foley RN, Gilbertson DT, Chen SC. United States renal data system public health surveillance of chronic kidney disease and end-stage renal disease. Kidney Int Suppl (2011). 2015;5(1):2–7.
4. Briet M, Burns KD. Chronic kidney disease and vascular remodelling: Molecular mechanisms and clinical implications. Clin Sci (Lond). 2012; 123(7):399–416.
5. Leopold JA. Vascular calcification: Mechanisms of vascular smooth muscle cell calcification. Trends Cardiovasc Med. 2015;25(4):267–274.
6. He F, Wang H, Ren WY, Ma Y, Liao YP, Zhu JH, et al. BMP9/COX-2 axial mediates high phosphate-induced calcification in vascular smooth muscle cells via Wnt/beta-catenin pathway. J Cell Biochem. 2018;119(3):2851–2863.
7. Yamamoto M. Vascular calcification - pathological mechanism and clinical application -. Vascular calcification as a clinical manifestation of bone-vascular axis. Clin Calcium. 2015;25(5):655–660.
8. Smith ER. Vascular calcification in uremia: New-age concepts about an old-age problem. Methods Mol Biol. 2016;1397:175–208.
9. Tonelli M, Curhan G, Pfeffer M, Sacks F, Thadhani R, Melamed ML, et al. Relation between alkaline phosphatase, serum phosphate, and all-cause or cardiovascular mortality. Circulation. 2009;120(18):1784–1792.
10. Li JW, Xu C, Fan Y, Wang Y, Xiao YB. Can serum levels of alkaline phosphatase and phosphate predict cardiovascular diseases and total mortality in individuals with preserved renal function? A systemic review and meta-analysis. PLoS One. 2014;9(7):e102276.
11. Olauson H, Vervloet MG, Cozzolino M, Massy ZA, Ureña Torres P, Larsson TE, et al. New insights into the FGF23-Klotho axis. Semin Nephrol. 2014;34(6):586–597.
12. Kurosu H, Ogawa Y, Miyoshi M, Yamamoto M, Nandi A, Rosenblatt KP, et al. Regulation of fibroblast growth factor-23 signaling by klotho. J Biol Chem. 2006;281(10):6120–6123.
13. Martín-Núñez E, Donate-Correa J, Muros-de-Fuentes M, Mora-Fernández C, Navarro-González JF. Implications of Klotho in vascular health and disease. World J Cardiol. 2014;6(12):1262–1269.
14. Feng JQ, Ward LM, Liu S, Lu Y, Xie Y, Yuan B, et al. Loss of DMP1 causes rickets and osteomalacia and identifies a role for osteocytes in mineral metabolism. Nat Genet. 2006;38(11):1310–1315.
15. Lu X, Hu MC. Klotho/FGF23 Axis in chronic kidney disease and cardiovascular disease. Kidney Dis (Basel). 2017;3(1):5–23.
16. Lim K, Lu TS, Molostvov G, Lee C, Lam FT, Zehnder D, et al. Vascular Klotho deficiency potentiates the development of human artery calcification and mediates resistance to fibroblast growth factor 23. Circulation. 2012;125(18):2243–2255.
17. Yao L, Sun YT, Sun W, Xu TH, Ren C, Fan X, et al. High phosphorus level leads to aortic calcification via beta-catenin in chronic kidney disease. Am J Nephrol. 2015;41(1):28–36.
18. Rong S, Zhao X, Jin X, Zhang Z, Chen L, Zhu Y, et al. Vascular calcification in chronic kidney disease is induced by bone morphogenetic protein-2 via a mechanism involving the Wnt/beta-catenin pathway. Cell Physiol Biochem. 2014;34(6):2049–2060.
19. Gu Q, Tian H, Zhang K, Chen D, Chen D, Wang X, et al. Wnt5a/FZD4 mediates the mechanical stretch-induced osteogenic differentiation of bone mesenchymal stem cells. Cell Physiol Biochem. 2018;48(1): 215–226.
20. Tang X, Wang Y, Fan Z, Ji G, Wang M, Lin J, et al. Klotho: A tumor suppressor and modulator of the Wnt/beta-catenin pathway in human hepatocellular carcinoma. Lab Invest. 2016;96(2):197–205.
21. Hu MC, Shi M, Zhang J, Quiñones H, Griffith C, Kuro-o M, et al. Klotho deficiency causes vascular calcification in chronic kidney disease. J Am Soc Nephrol. 2011;22(1):124–136.
22. Zhao Y, Zhao MM, Cai Y, Zheng MF, Sun WL, Zhang SY, et al. Mammalian target of rapamycin signaling inhibition ameliorates vascular calcification via Klotho upregulation. Kidney Int. 2015;88(4):711–721.
23. Jimbo R, Kawakami-Mori F, Mu S, Hirohama D, Majtan B, Shimizu Y, et al. Fibroblast growth factor 23 accelerates phosphate-induced vascular calcification in the absence of Klotho deficiency. Kidney Int. 2014;85(5):1103–1111.
24. Massy ZA, Drueke TB. Vascular calcification. Curr Opin Nephrol Hypertens. 2013;22(4):405–412.
25. Desjardins L, Liabeuf S, Renard C, Lenglet A, Lemke HD, Choukroun G, et al. FGF23 is independently associated with vascular calcification but not bone mineral density in patients at various CKD stages. Osteoporos Int. 2012;23(7):2017–2025.
26. McCarty MF, DiNicolantonio JJ. The molecular biology and pathophysiology of vascular calcification. Postgrad Med. 2014;126(2): 54–64.
27. Wu M, Rementer C, Giachelli CM. Vascular calcification: An update on mechanisms and challenges in treatment. Calcif Tissue Int. 2013; 93(4):365–373.
28. Rensen SS, Doevendans PA, van Eys GJ. Regulation and characteristics of vascular smooth muscle cell phenotypic diversity. Neth Heart J. 2007;15(3):100–108.
29. Mori K, Shioi A, Jono S, Nishizawa Y, Morii H. Dexamethasone enhances in vitro vascular calcification by promoting osteoblastic differentiation of vascular smooth muscle cells. Arterioscler Thromb Vasc Biol. 1999;19(9):2112–2118.
30. Giachelli CM. Vascular calcification: in vitro evidence for the role of inorganic phosphate. J Am Soc Nephrol. 2003;14(9):S300–S304.
31. Liu J, Zhang L, Zhou Y, Zhu D, Wang Q, Hao L, et al. Aberrant activation of Wnt pathways in arteries associates with vascular calcification in chronic kidney disease. Int Urol Nephrol. 2016;48(8): 1313–1319.
32. Deng D, Diao Z, Han X, Liu W. Secreted frizzled-related protein 5 attenuates high phosphate-induced calcification in vascular smooth muscle cells by inhibiting the Wnt/-catenin pathway. Calcif Tissue Int. 2016;99(1):66–75.

How to cite this article: Chen Y-X, Huang C, Duan Z-B, Xu C-Y, Chen Y. Klotho/FGF23 axis mediates high phosphate-induced vascular calcification in vascular smooth muscle cells via Wnt7b/β-catenin pathway. *Kaohsiung J Med Sci*. 2019;35: 393–400. https://doi.org/10.1002/kjm2.12072